Oncology Treatment Discovery, 2025, Volume 3, Issue 3
http://ojs.bbwpublisher.com/index.php/OTD
Online ISSN: 2981-8079
Print ISSN: 3083-4996

Investigation of Potential Biological Mechanisms Linking Blood Lipids and Head and Neck Squamous Cell Carcinoma

Aoxiong Zhou[1]*, Jiahao Chen[2], Yumeng Ou[1], Jinhai Wu[3]

[1]Department of Radiotherapy V, Guangzhou Institute of Cancer Research, the Affiliated Cancer Hospital, Guangzhou Medical University, Guangzhou, Guangdong, China

[2]Department of Hepatobiliary Surgery, Guangzhou Institute of Cancer Research, the Affiliated Cancer Hospital, Guangzhou Medical University, Guangzhou, Guangdong, China

[3]Department of Urology, Guangzhou Institute of Cancer Research, the Affiliated Cancer Hospital, Guangzhou Medical University, Guangzhou, Guangdong, China

**Author to whom correspondence should be addressed.*

Abstract: *Background:* Head and neck squamous cell carcinoma (HNSCC) is a common malignancy with a heterogeneous etiology. Circulating total cholesterol (TC), apolipoprotein A-I (ApoA-I), and low-density lipoprotein cholesterol (LDL-C) may influence tumorigenesis via metabolic, inflammatory, and immune pathways. The causal relationship and molecular mechanisms remain unclear. This study systematically evaluated lipid-related genetic variants and HNSCC risk. *Methods:* Two-sample Mendelian randomization (MR) using genome-wide association study (GWAS) data assessed causal effects of TC, ApoA-I, and LDL-C on head and neck cancer (HNC). Significant single-nucleotide polymorphisms (SNPs) were functionally annotated and subjected to pathway enrichment. Candidate genes were analyzed in GEPIA2, TIMER3.0, and cBioPortal for differential expression (DE), survival, immune infiltration, and clinical stage associations. *Results:* MR revealed no significant causal effects (P>0.05). Positive effect group SNPs are enriched in cytochrome P450 (CYP450)-mediated xenobiotic metabolism; negative effect group SNPs are enriched in monocarboxylic acid and alcohol metabolism pathways, suggesting protective metabolic adaptation. DE analysis showed ADH1B downregulation and FADS1/2, PARP9, and SEMA7A upregulation. Immune infiltration linked these genes to $CD8^+$ T cells, M1/M2 macrophages, regulatory T cells (Treg), cancer-associated fibroblasts (CAF), and NK cells, with ADH1B downregulation associated with immunotherapy response. ALDH1A2, EVI5, and LCAT, though not DE, exhibited prognostic value, with expression increasing in advanced stages. *Conclusion:* Lipid-related variants may influence HNSCC via opposing mechanisms: CYP450/inflammation versus metabolic adaptation/alcohol pathways. ADH1B and FADS1/2, PARP9, SEMA7A regulate tumor metabolism and immune microenvironment; ALDH1A2, EVI5, and LCAT hold prognostic potential. These findings provide mechanistic insight and candidate molecular targets for HNSCC prediction and intervention.

Keywords: Lipids; HNSCC; Functional enrichment; Immune infiltration; Prognostic biomarkers

Online publication: October 16, 2025

1. Introduction

Head and neck squamous cell carcinoma (HNSCC) is one of the most common malignancies worldwide and imposes a significant public health burden. HNSCC accounts for hundreds of thousands of new cases and deaths annually worldwide, with highly heterogeneous etiology and carcinogenic mechanisms [1]. Beyond traditional risk factors such as smoking, alcohol consumption, and HPV infection, metabolic abnormalities and alterations in lipid profiles have recently attracted increasing attention [2]. Circulating lipids, which play essential roles in energy metabolism, cell membrane synthesis, and signaling pathways, are thought to contribute to tumor initiation and progression through inflammation, immune modulation, and endocrine mechanisms [3,4].

Multiple clinical and epidemiological studies have reported associations between circulating lipids (total cholesterol [TC], low-density lipoprotein [LDL], high-density lipoprotein [HDL], triglycerides [TG]) and apolipoproteins (ApoA-I, ApoB) with the risk or prognosis of head and neck tumors [5–9]. Some studies have further suggested that preoperative or treatment-period lipid and ApoA-I levels may predict responses to immunotherapy or chemoradiotherapy and survival outcomes [10]. These observational findings indicate measurable signals between "lipid levels and tumor phenotypes." However, due to confounding factors (e.g., smoking, nutritional status, concomitant medications—particularly statins), reverse causation, and differences in sample size or tumor subtypes, observational evidence alone is insufficient to establish causality.

Accordingly, we designed a multi-layered research framework: first, two-sample Mendelian randomization (MR) analyses were conducted using publicly available GWAS data to assess the causal effects of high cholesterol, ApoA-I and low-density lipoprotein cholesterol (LDL-C) on head and neck cancer risk; subsequently, single nucleotide polymorphisms (SNPs) exhibiting consistent effect directions in both exposures and outcomes and reaching statistical significance were selected for functional annotation and pathway enrichment analyses to explore the associated metabolic and signaling networks; finally, the identified genes were integrated into multi-omics and online database platforms (GEPIA2, TIMER3.0, and cBioPortal) to perform differential expression, survival, immune infiltration, and clinicopathological association analyses, thereby elucidating potential links between circulating lipids, genetic variation, molecular mechanisms, and clinical phenotypes. This integrative research strategy aims to provide more reliable and systematic evidence regarding the causal relationship between lipid metabolism and HNSCC risk, as well as the underlying molecular pathways, offering new insights for future clinical prediction and intervention.

2. Materials and methods

2.1. Overall study design

The overall study design comprised three sequential steps:

(1) Conducting two-sample MR analyses using publicly available GWAS summary data to evaluate the potential causal associations of high cholesterol, ApoA-I, and LDL-C with head and neck cancer risk (HNC);

(2) Based on the significant SNPs identified from the MR analyses, variants exhibiting consistent effect directions across both exposures and outcomes and reaching statistical significance were selected, categorized into positive and negative effect groups, and subjected to functional annotation and enrichment analyses to explore the underlying biological pathways;

(3) All candidate genes were then integrated into multi-omics and online database platforms, including GEPIA2, TIMER3.0, and cBioPortal, to perform differential expression, survival, immune infiltration,

and clinicopathological association analyses.

2.2. Data sources

This study employed a two-sample MR approach to assess the potential causal relationships between circulating lipid-related exposures and HNC risk. The exposures included high cholesterol (ebi-a-GCST90029021), ApoA-I (ieu-b-107), and LDL-C (ieu-b-110), while the outcome was head and neck cancer (ieu-b-4912). The GWAS summary statistics for these exposures and the outcome were retrieved and downloaded from the OpenGWAS platform (https://gwas.mrcieu.ac.uk/) [11]. All data were derived from previously published studies with appropriate ethical approvals; therefore, no additional ethical approval was required for this study.

2.3. SNP dressing by screening

SNPs significantly associated with high cholesterol, ApoA-I, and LDL-C ($p < 5 \times 10^{-8}$) were selected. SNPs in linkage disequilibrium ($r^2 < 0.001$, window < 10,000 kb) were excluded to retain independent variants for subsequent analyses. Subsequently, the F statistic for each SNP was calculated to ensure instrument strength (F > 10), and weak instruments were excluded. Finally, the validity and robustness of the selected instruments were further assessed using the MR Steiger filter and the MR-PRESSO test.

For the primary MR analyses, SNPs present in both exposures and outcome with consistent effect directions (i.e., both beta.exposure and beta.outcome positive or both negative) and reaching statistical significance in both ($P < 0.05$) were retained as the main analysis set. These SNPs were then categorized into positive and negative effect groups according to effect direction and retained for subsequent functional annotation and enrichment analyses.

2.4. SNP function annotation and gene localization

All SNPs from each group were input into the Ensembl Variant Effect Predictor (VEP; https://www.ensembl.org/Tools/VEP) for functional annotation to determine their potential regulatory effects, functional categories, and the candidate genes they mapped to [12]. VEP is a powerful and flexible tool that annotates the potential biological impact of genomic variants and provides detailed information regarding variant positions, implicated genes, and their possible functions, thereby enabling the identification of genes mapped by SNPs in the positive and negative effect groups. The genes were then organized into two independent gene sets, corresponding to the positive and negative effect groups; finally, all genes mapped by the SNPs were combined into a comprehensive target gene set for subsequent analyses.

2.5. Enrichment analysis

Metascape (https://metascape.org) is an integrated bioinformatics platform [13] that incorporates over 40 distinct biological databases and offers various functional analyses, including interactive analysis and gene annotation. Pathway and functional enrichment analyses were performed separately for the positive and negative gene sets using Metascape, extracting significantly enriched biological processes, signaling pathways, and cellular components.

2.6. Differential expression and survival analysis

GEPIA2 (http://gepia.cancer-pku.cn/index.html) is a comprehensive online analysis platform [14] that leverages RNA-sequencing data from The Cancer Genome Atlas (TCGA) and the Genotype-Tissue Expression (GTEx) projects. All candidate genes mapped by SNPs were input into GEPIA2 for differential expression analysis (tumor

vs. normal) and survival analysis (overall survival and disease-free survival) using the TCGA HNSC dataset. Differential expression analysis was conducted using normalized RNA-seq TPM data, with statistical significance assessed via an ANOVA model. Survival analysis was performed using the Kaplan–Meier method, with samples stratified by median expression levels, and significance tested using the log-rank test.

2.7. Correlation between immune infiltration and immunotherapy

Genes showing significant differential expression in GEPIA2 were further evaluated in TIMER3.0 (http://timer.cistrome.org/) for their associations with the tumor immune microenvironment [15]. TIMER3.0 provides comprehensive immune infiltration analysis and assessment of immunotherapy effects. Analyses included correlations between candidate gene expression and various immune cell types, such as $CD8^+$ T cells, regulatory T cells (Tregs), macrophage subtypes (M0, M1, and M2), cancer-associated fibroblasts (CAFs), neutrophils, natural killer (NK) cells, and myeloid-derived suppressor cells (MDSCs), along with an immunotherapy response prediction module to explore the potential immunotherapeutic relevance of these genes.

2.8. Analysis of clinical pathological staging

cBioPortal for Cancer Genomics (http://cbioportal.org) is an open-access cancer genomics resource [16] that provides integrated views of cancer genomic datasets along with associated clinical information. Genes showing significant prognostic associations in survival analyses were queried in cBioPortal to assess the relationships between mRNA expression levels and clinical features, including pathological stage and mutation status, within the TCGA-HNSC dataset. Gene expression distributions were extracted following the default cBioPortal workflow and compared across different pathological stages.

2.9. Statistical analysis

Primary MR analyses were conducted using R version 4.5.1 with the TwoSampleMR package, employing methods such as MR-IVW, weighted median, and MR-Egger, along with MR-PRESSO to detect potential pleiotropy and outliers [17]. Functional annotation, enrichment, differential expression, immune infiltration, and pathological stage analyses were all performed using the default or recommended parameters of each platform. All statistical tests were two-sided, with $P < 0.05$ considered statistically significant, and multiple testing corrections applied when appropriate.

3. Results

3.1. Mendel randomized analysis of blood lipids and head and neck cancer

This study employed a two-sample MR approach to evaluate the potential causal effects of lipid-related exposures on HNC risk. The results indicated that high cholesterol, ApoA-I, and LDL-C were not significantly associated with head and neck cancer risk (**Table 1**). Estimates obtained from weighted median, MR-Egger, simple mode, and weighted mode methods were directionally consistent, with all P values > 0.05. The concordant effect directions across different MR methods, coupled with the lack of statistical significance, suggest an absence of robust direct causal evidence linking high cholesterol, ApoA-I, and LDL-C levels to head and neck cancer risk.

Table 1. Mendelian randomization analysis of blood lipids and head and neck cancers

Outcome	Exposure	Method	nSNP	B	se	p - value
Head and neck cancer	High cholesterol	MR Egger	75	-2.01E-03	3.65E-03	0.58
		Weighted median	75	3.22E-03	3.18E-03	0.31
		Inverse variance weighted	75	7.79E-04	2.15E-03	0.72
		Simple mode	75	5.56E-03	5.72E-03	0.33
		Weighted mode	75	2.31E-03	3.43E-03	0.50
	Apolipoprotein A-I	MR Egger	292	2.83E-04	4.66E-04	0.54
		Weighted median	292	9.87E-04	5.44E-04	0.07
		Inverse variance weighted	292	-9.88E-06	3.09E-04	0.97
		Simple mode	292	-6.92E-04	1.34E-03	0.61
		Weighted mode	292	6.82E-04	5.39E-04	0.21
	LDL cholesterol	MR Egger	177	1.38E-04	3.95E-04	0.73
		Weighted median	177	5.43E-04	4.62E-04	0.24
		Inverse variance weighted	177	3.83E-04	2.98E-04	0.20
		Simple mode	177	-1.12E-04	9.61E-04	0.91
		Weighted mode	177	2.66E-04	3.70E-04	0.47

3.2. SNP functional annotation analysis

To further investigate the potential biological mechanisms through which lipid-related genetic variants may influence head and neck cancer, we performed functional annotation on SNPs selected from the MR analysis results. First, based on the effect direction (i.e., concordant beta values for exposure and outcome) and statistical significance ($P < 0.05$), SNPs were classified into a positive effect group (beta > 0, $n = 10$) and a negative effect group (beta < 0, $n = 8$). Subsequently, SNPs from each group were input into the VEP for functional annotation and gene mapping. Functional annotation revealed that the positive effect group SNPs mapped to 11 candidate genes, while the negative effect group SNPs also mapped to 11 candidate genes. The annotation process included the genomic loci of the SNPs, variant types (e.g., exonic nonsynonymous, intronic, regulatory region variants), and predictions of potential regulatory functions.

3.3. Functional enrichment analysis

Considering the potential involvement of complex multi-pathway mechanisms linking lipid metabolism to tumorigenesis, we further performed functional annotation and pathway enrichment analyses on genes grouped by the direction of their beta values.

3.3.1. Positive group SNP enrichment analysis results

Genes mapped from the positive effect group SNPs were significantly enriched in the “Drug metabolism, cytochrome P450” pathway (KEGG), as well as Gene Ontology (GO) biological processes, including “response to xenobiotic stimulus” and “regulation of catalytic activity” (**Figure 1**). These findings suggest that these genes are primarily involved in the metabolism and clearance of exogenous chemicals, such as drugs and environmental carcinogens, and are closely associated with regulating enzymatic activity. DisGeNET disease

phenotype enrichment analysis indicated that these genes were significantly associated with various inflammatory and immune-related disorders (**Figure 2**), including "Allergic Reaction," "Alcohol-Induced Disorders," and "Neutrophilia," and were also highly relevant to tumor phenotypes, such as "Malignant neoplasm of larynx," "Carcinoma of larynx," and "Laryngeal Squamous Cell Carcinoma." PaGenBase tissue-specific expression analysis showed that this gene set was enriched in liver tissue (Count = 3, 27%, Log10(P) = -2.80), suggesting a specific role for these genes in hepatic metabolic processes. Transcription factor target enrichment analysis revealed a significant enrichment of DLX6 target genes (Count = 4, 36%, Log10(P) = -4.40). DLX6 is a transcription factor involved in embryonic development, and its antisense RNA (DLX6-AS1) has been reported to promote cell proliferation and metastasis in laryngeal and other head and neck cancers.

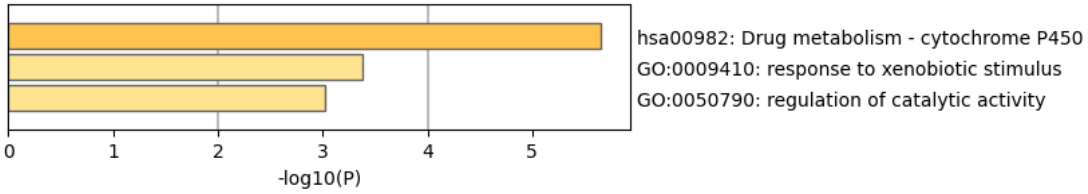

Figure 1. Pathway and process enrichment analysis (+SNP).

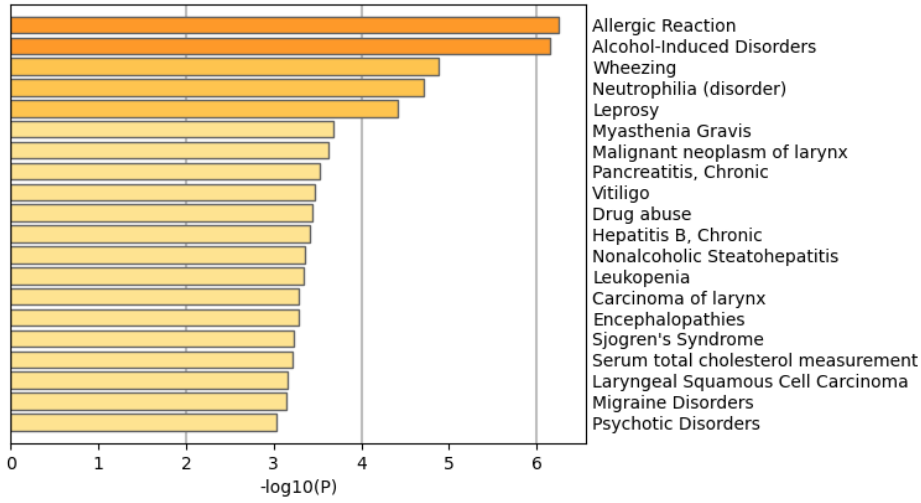

Figure 2. DisGeNET disease association analysis (+SNP).

3.3.2. Negative group SNP enrichment analysis results

Genes mapped from the negative effect group SNPs were primarily enriched in metabolic and adaptive processes, including the "monocarboxylic acid biosynthetic process," "alcohol metabolic process," and "response to nutrient levels" (**Table 2**). Among these, monocarboxylic acid metabolism showed the most significant enrichment, encompassing the production and utilization of key metabolites such as lactate and short-chain fatty acids, suggesting a potential role in energy metabolism and tumor microenvironment regulation. DisGeNET disease phenotype enrichment (**Figure 3**) indicated that these genes were closely associated with multiple lipid-related traits, including HDL, LDL, total cholesterol, triglycerides, and metabolic disorders such as hypertriglyceridemia and dyslipidemia. Additionally, they were significantly associated with glucose levels, hematological parameters

(e.g., white blood cell count, hemoglobin), and inflammatory markers (e.g., C-reactive protein, serum albumin). Transcription factor regulatory enrichment highlighted the target gene sets of ZNF507 and ZNF589. These two zinc finger transcription factors are widely involved in gene transcription regulation, chromatin structure maintenance, and cell fate determination, and their downstream regulatory networks may serve as a bridge between lipid metabolism regulation and tumor risk modulation.

Table 2. Pathway and process enrichment analysis (-SNP)

GO	Category	Description	Count	%	Log10(P)	Log10(q)
GO:0072330	GO Biological Processes	monocarboxylic acid biosynthetic process	4	36.36	-6.41	-2.07
GO:0006066	GO Biological Processes	alcohol metabolic process	3	27.27	-3.74	-0.40
GO:0031667	GO Biological Processes	response to nutrient levels	3	27.27	-3.08	0.00

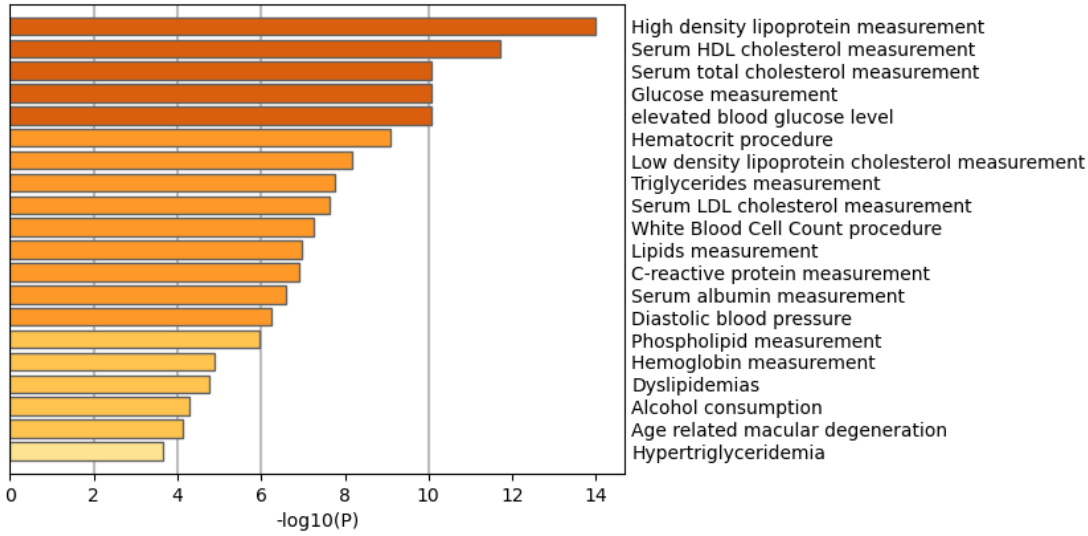

Figure 3. DisGeNET disease association analysis (-SNP).

3.4. Differentially expressed genes

To further investigate the potential roles of genes mapped from relevant SNPs in head and neck squamous cell carcinoma (HNSC), we integrated all genes mapped from both positive and negative effect SNPs as target genes for differential expression analysis. Gene expression data were obtained from the GEPIA2 database, comparing expression levels between HNSC tumor tissues and normal tissues. The analysis revealed that among all target genes, ADH1B, FADS1, FADS2, PARP9, and SEMA7A exhibited significant differential expression in HNSC tissues. Specifically, ADH1B was significantly downregulated in tumor tissues compared to normal tissues, whereas FADS1, FADS2, PARP9, and SEMA7A were significantly upregulated in tumor tissues, exhibiting higher transcriptional levels relative to normal tissues (**Figure 4**). These findings suggest that ADH1B may play a potential protective role in tumorigenesis or tumor-suppressive mechanisms, whereas FADS1, FADS2, PARP9, and SEMA7A may be associated with tumor progression.

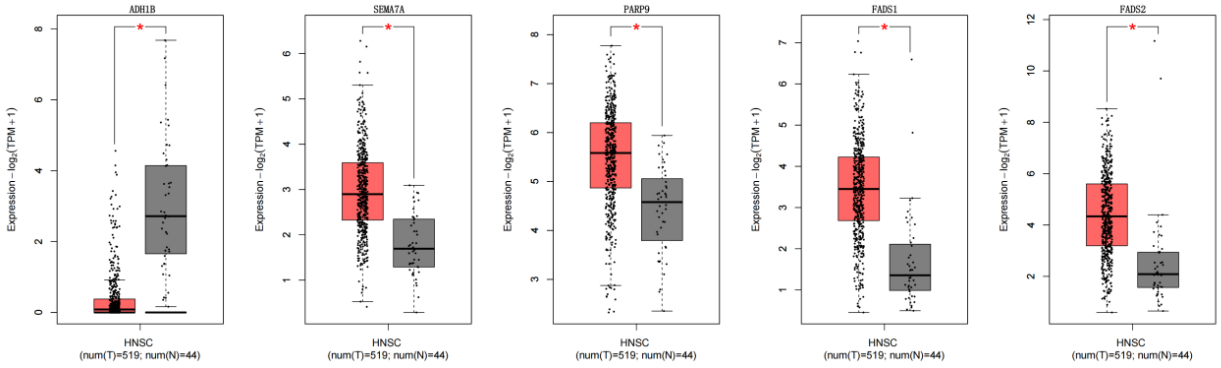

Figure 4. FADS1, FADS2, PARP9 and SEMA7A differential expression analysis.

3.5. Immune infiltration analysis and immune therapy response

3.5.1. Correlation between differentially expressed genes and tumor immune infiltration

Using TIMER3.0 and multiple immune estimation tools, we analyzed the correlations between ADH1B, FADS1, FADS2, PARP9, and SEMA7A and immune cell infiltration, revealing that all these genes were significantly associated with the infiltration levels of multiple immune cell types. ADH1B expression was positively correlated with $CD8^+$ T cells (Rho = 0.292, $p = 4.38 \times 10^{-11}$), M1 macrophages (Rho = 0.332, $p = 4.39 \times 10^{-14}$), and NK cells (Rho = 0.309, $p = 2.51 \times 10^{-12}$), but negatively correlated with MDSCs (Rho = -0.136, $p = 2.6 \times 10^{-3}$) and neutrophils (Rho = -0.257, $p = 7.96 \times 10^{-9}$) (**Figure 5**). FADS1 was significantly positively correlated with cancer-associated fibroblasts (CAF, Rho = 0.382, $p = 1.68 \times 10^{-18}$), MDSCs (Rho = 0.253, $p = 1.28 \times 10^{-8}$), M2 macrophages (Rho = 0.336, $p = 2.14 \times 10^{-14}$), and Tregs (Rho = 0.20, $p = 7.84 \times 10^{-6}$), while negatively correlated with $CD8^+$ T cells (Rho = -0.444, $p = 4.33 \times 10^{-25}$) (**Figure 6**). FADS2 exhibited strong positive correlations with CAF (Rho = 0.405, $p = 8.18 \times 10^{-21}$), M2 macrophages (Rho = 0.41, $p = 2.67 \times 10^{-21}$), and Tregs (Rho = 0.303, $p = 7.06 \times 10^{-12}$), while negatively correlating with $CD8^+$ naïve T cells (Rho = -0.316, $p = 8.27 \times 10^{-13}$) and NK cells (Rho = -0.226, $p = 4.12 \times 10^{-7}$) (**Figure 7**). PARP9 was strongly correlated with M1 macrophages (Rho = 0.565, $p = 1.34 \times 10^{-42}$), M2 macrophages (Rho = 0.303, $p = 7.37 \times 10^{-12}$), Tregs (Rho = 0.381, $p = 2.05 \times 10^{-18}$), neutrophils (Rho = 0.58, $p = 2.27 \times 10^{-45}$), and NK cells (Rho = 0.433, $p = 9.04 \times 10^{-24}$), while negatively correlating with $CD8^+$ naïve T cells (Rho = -0.322, $p = 2.85 \times 10^{-13}$) (**Figure 8**). SEMA7A was positively correlated with CAF (Rho = 0.315, $p = 8.94 \times 10^{-13}$), M0/M2 macrophages (Rho = 0.345, $p = 3.84 \times 10^{-15}$; Rho = 0.199, $p = 9.00 \times 10^{-6}$), and neutrophils (Rho = 0.365, $p = 6.34 \times 10^{-17}$), while negatively correlated with $CD8^+$ T cells (Rho = -0.159, $p = 4.07 \times 10^{-4}$) and activated NK cells (Rho = -0.193, $p = 1.65 \times 10^{-5}$) (**Figure 9**).

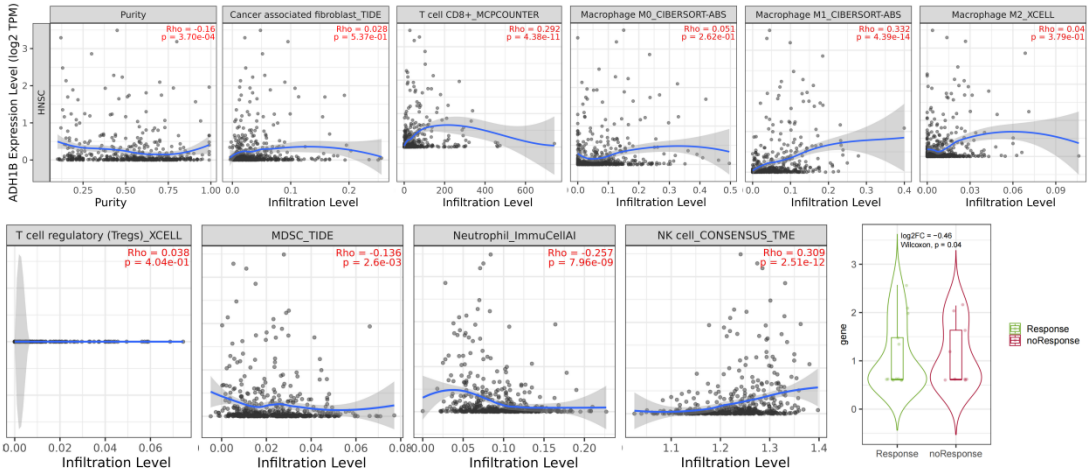

Figure 5. ADH1B Immune infiltration analysis and immune response to therapy.

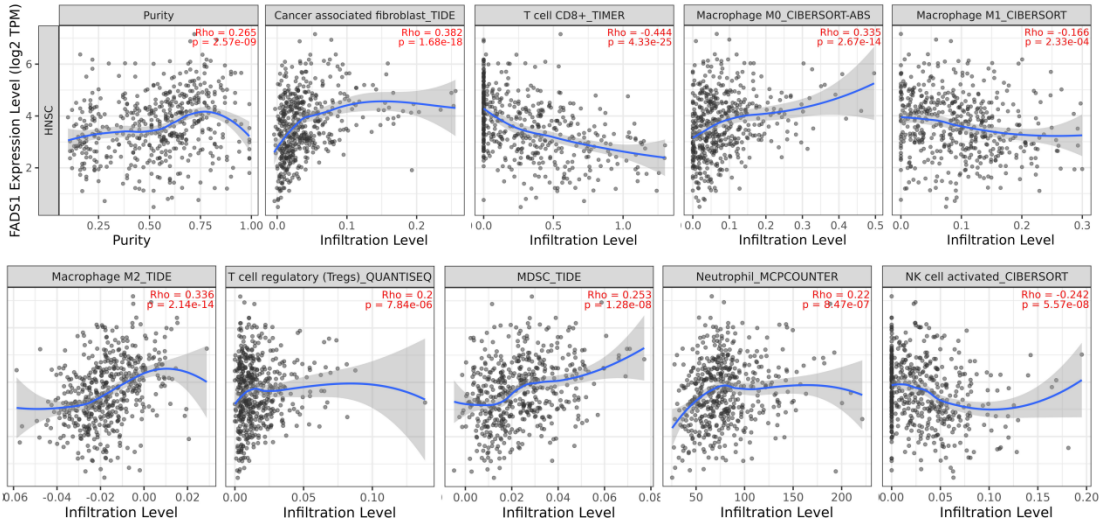

Figure 6. FADS1 Immune infiltration analysis.

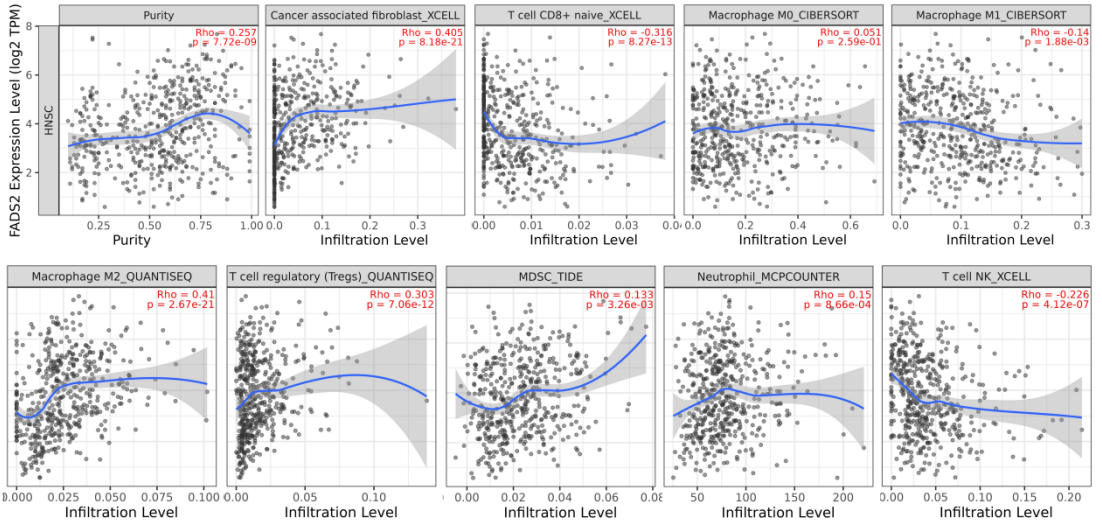

Figure 7. FADS2 Immune infiltration analysis.

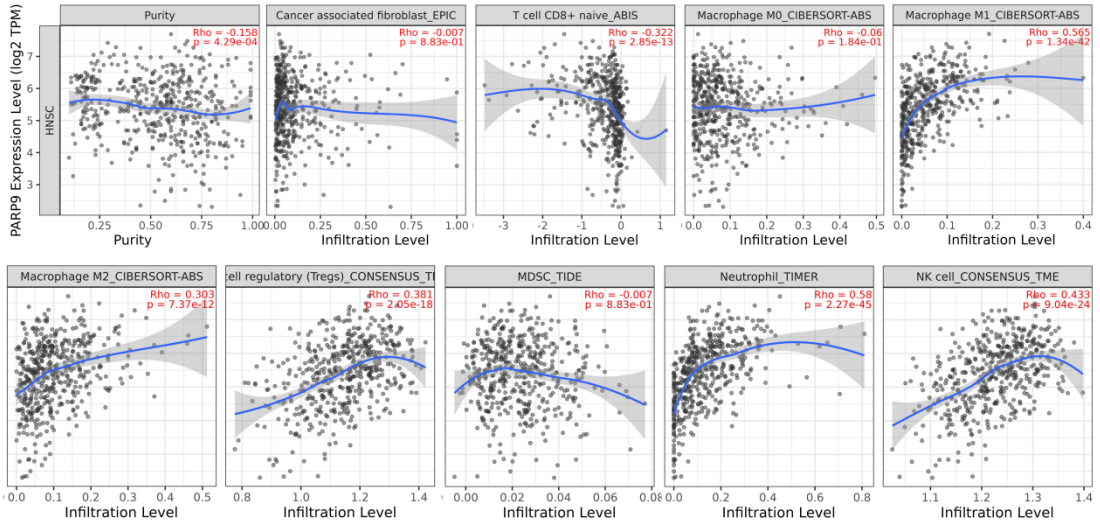

Figure 8. ADH1B Immune infiltration analysis.

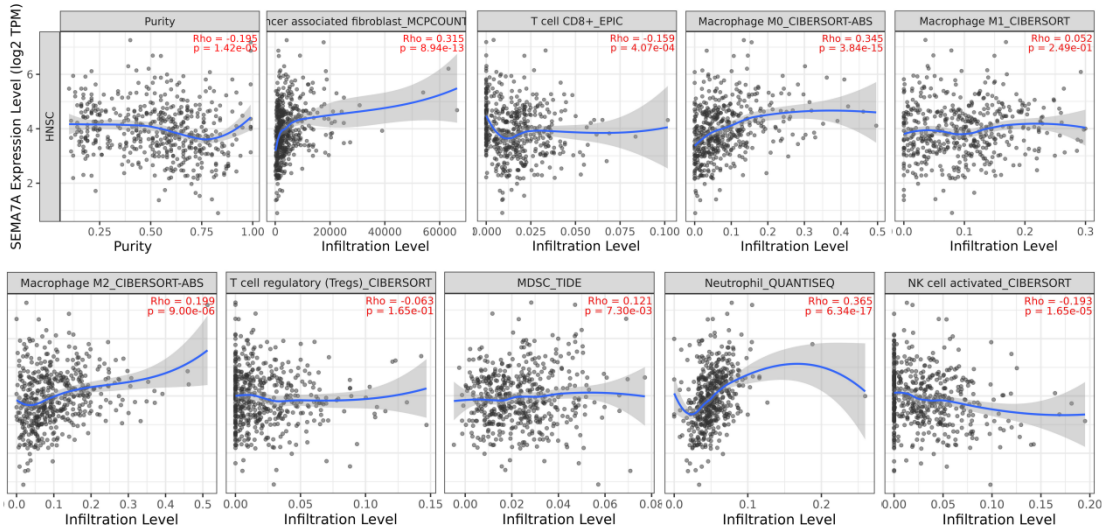

Figure 9. SEMA7A Immune infiltration analysis.

3.5.2. Relationship between genes and immune response to therapy

In the immunotherapy response analysis, ADH1B expression was significantly lower in responders compared with non-responders (log2FC = -0.46, p = 0.04). Further analysis using the Immunotherapy_Gene module revealed that only ADH1B exhibited a statistically significant association with immunotherapy response, whereas the remaining genes did not show significant correlations (**Figure 5**).

3.5. Correlation analysis between survival analysis and clinical pathological staging

To further investigate the clinical relevance of genes that did not exhibit significant differential expression but showed prognostic significance in survival analysis, we integrated the survival results from GEPIA2 with pathological stage data from cBioPortal (**Figure 10**). The results indicated that ALDH1A2, EVI5, and LCAT, although not significantly differentially expressed between tumor and normal tissues, exhibited statistically significant associations with OS or DFS. ALDH1A2 showed significant associations with OS (log-rank p =

0.014, *HR* = 1.4, *p* = 0.015) and DFS (log-rank *p* = 0.037, *HR* = 1.4, *p* = 0.038). Its mRNA expression gradually increased with tumor stage (from stage I to stage IVA), with stage IVA samples exhibiting a more concentrated and higher expression distribution. Mutation types included splice variants, missense mutations, shallow deletions, and gene amplifications, with a higher proportion of high-expression samples observed in stage IVA.

EVI5 was significantly associated with OS (log-rank *p* = 0.018, *HR* = 0.73, *p* = 0.019), suggesting that its high expression may confer a protective effect. Stage-wise analysis showed that EVI5 mRNA expression gradually increased from stage I to stage IVA, with overall higher expression levels in stage IVA. Mutation types included splice variants, missense mutations, truncating mutations, in-frame mutations, amplifications, and deletions, with an increased proportion of high-expression samples in stage IVA.

LCAT was significantly associated with DFS (log-rank *p* = 0.022, *HR* = 1.5, *p* = 0.023). Its mRNA expression exhibited a broader distribution in stage IVA, with mutation types including gene amplifications, gains, and shallow deletions. Although its stage-related expression was less pronounced than that of ALDH1A2 and EVI5, some stage IVA samples exhibited high expression levels.

Although ALDH1A2, EVI5, and LCAT did not show significant differential expression, they were closely associated with tumor progression stages and molecular alterations, and exhibited potential prognostic value. Notably, in advanced stage (stage IVA), all three genes displayed more prominent expression patterns, suggesting their involvement in HNSCC progression and potential as clinical prognostic biomarkers.

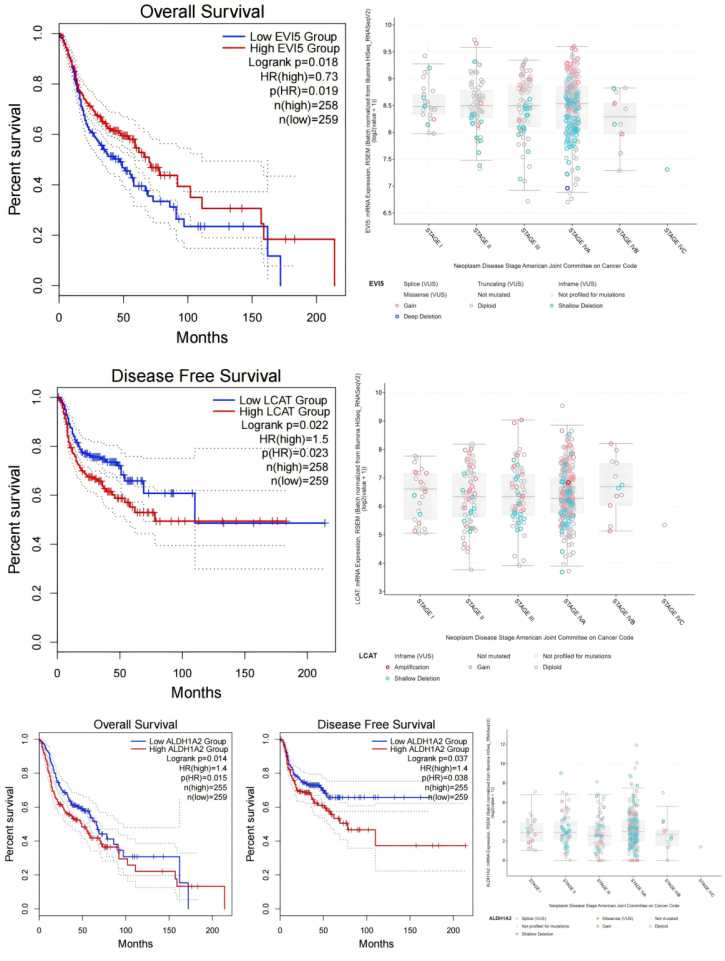

Figure 10. Survival analysis of ALDH1A2, EVI5 and LCAT and correlation with pathological stage.

4. Discussion

This study systematically evaluated the potential causal relationship between blood lipid–related exposures (high cholesterol, ApoA-I, and LDL-C) and head and neck cancer risk using a two-sample Mendelian randomization (MR) approach. Overall, the MR analyses did not reveal a significant causal effect of these lipid traits on HNC risk ($P > 0.05$). It should be noted that the outcome in this MR analysis encompassed broad HNC, including various anatomical sites and histological subtypes, rather than being restricted to head and neck HNSCC. Consequently, potential heterogeneity and the inclusion of other cancer subtypes may partially obscure the localized effects of blood lipid levels on HNSCC.

4.1. Potential mechanisms and enrichment analysis of SNPs associated with blood lipids

The genes mapped by positive effect group SNPs were significantly enriched in cytochrome P450 (CYP450)–related metabolic pathways and xenobiotic metabolism processes, suggesting that blood lipid–associated genetic variants may modulate the function of hepatic CYP450 enzymes, thereby altering the metabolic capacity for exogenous chemicals such as tobacco carcinogens and ethanol metabolites. Previous studies have demonstrated that CYP family members (e.g., CYP1A1, CYP2E1) can convert polycyclic aromatic hydrocarbons and ethanol metabolites into reactive carcinogens, increasing the risk of DNA damage [18]. Moreover, as the liver serves as the central hub for systemic metabolism, differential expression of these genes may influence the distribution and accumulation of blood lipids and carcinogenic metabolites in circulation, thereby modifying exposure levels in head and neck mucosal tissues. DisGeNET analyses further indicated that genes mapped by positive effect group SNPs are significantly associated with laryngeal cancer and other head and neck malignancies. Enrichment of DLX6 target genes suggests that transcription factor networks may promote malignant behavior by regulating cellular differentiation and proliferation. Notably, DLX6-AS1 has been reported to be overexpressed in laryngeal cancer tissues and associated with tumor progression and metastasis [19], which aligns closely with the enrichment results of the positive effect group SNPs in this study.

Conversely, genes mapped by negative effect group SNPs were enriched in monocarboxylic acid metabolism, alcohol metabolism, and nutrient response pathways. Key components of monocarboxylic acid metabolism, including lactate and short-chain fatty acids, not only participate in energy metabolism but also function as signaling molecules within the tumor microenvironment to modulate immune cell activity. Variants in these genes may enhance metabolic adaptability under hyperlipidemic or metabolic stress conditions, potentially exerting protective effects against HNSCC. The enrichment of alcohol metabolism–related genes is particularly noteworthy, as acetaldehyde, an intermediate of ethanol metabolism, is a well-established carcinogen [20]; genetic variants that accelerate acetaldehyde clearance could mitigate mucosal damage in the head and neck. Genes mapped by negative effect group SNPs were also associated with multiple lipid and inflammatory biomarkers, suggesting a role in maintaining lipid homeostasis and modulating inflammation. Enrichment of ZNF507 and ZNF589 target genes reveals a potential transcriptional regulatory network [21]; these zinc finger transcription factors play pivotal roles in chromatin remodeling and gene expression regulation, potentially bridging lipid metabolism and tumor risk.

Taken together, the enrichment analyses of positive and negative effect group SNPs indicate that blood lipid levels and HNSCC/HNC risk may be co-regulated through two opposing mechanisms. On one hand, lipid-related genetic variants may enhance carcinogen effects via CYP450 metabolism and inflammatory pathways, increasing tumor risk. On the other hand, certain genetic backgrounds may confer metabolic adaptability and enhanced

ethanol metabolism, thereby buffering or mitigating this risk. The counteracting effects of these mechanisms may explain the absence of significant causal associations observed in the overall MR analysis. Furthermore, the broad HNC outcome used in MR analyses may introduce interference from other cancer subtypes, further obscuring the localized effects on HNSCC.

4.2. Differential expression is associated with immune microenvironment

Differential expression analysis of candidate genes mapped by the SNPs revealed that ADH1B was downregulated in HNSC tissues, whereas FADS1, FADS2, PARP9, and SEMA7A were significantly upregulated in tumors. This suggests a potential protective role for ADH1B, while the other genes may be implicated in tumor progression. Previous studies have demonstrated that ADH1B modulates the rate of alcohol metabolism, influencing acetaldehyde accumulation and DNA damage risk [22], and its polymorphisms are closely associated with HNSCC susceptibility [23], consistent with the differential expression patterns observed in the present study. FADS1 and FADS2, as fatty acid desaturases, participate in polyunsaturated fatty acid biosynthesis, potentially regulating tumor cell membrane fluidity and signal transduction, while also influencing the immune microenvironment via M2 macrophage polarization [24]. Upregulation of FADS2 promotes unsaturated fatty acid synthesis, thereby enhancing tumor cell proliferation and chemoresistance [25,26]. Although evidence linking PARP9 to HNSC is limited, studies indicate that it is involved in DNA damage response and cell survival signaling, coordinating protein interactions to support cancer cell viability [27]. Aberrant glycosylation of SEMA7A can facilitate the formation of an immunosuppressive microenvironment, promoting tumor immune evasion [28].

Our immune infiltration analysis showed that ADH1B expression positively correlated with $CD8^+$ T cells, M1 macrophages, and NK cells, but negatively correlated with MDSCs and neutrophils, suggesting that ADH1B may exert protective effects by enhancing anti-tumor immunity. In contrast, FADS1, FADS2, PARP9, and SEMA7A were positively associated with cancer-associated fibroblasts, M2 macrophages, and regulatory T cells, while negatively associated with $CD8^+$ T cells and NK cells, indicating that these genes may promote tumor progression by modulating an immunosuppressive microenvironment. These findings fill a gap in the current HNSC research by providing integrated immune correlation analysis. Furthermore, immunotherapy response analysis revealed that ADH1B was significantly downregulated in responders compared to non-responders, suggesting its potential utility as a predictive biomarker for immunotherapy efficacy. This observation extends existing knowledge on immunotherapy biomarkers and highlights the clinical relevance of these candidate genes in therapeutic response.

4.3. Correlation between clinical pathological stage and prognosis

Integrating differential expression and survival analyses, ALDH1A2, EVI5, and LCAT did not exhibit significant expression differences between tumor and normal tissues in our HNSC dataset, yet al.l showed statistically significant associations with OS or DFS. ALDH1A2 was significantly associated with both DFS and OS, with expression levels increasing alongside tumor stage; in advanced-stage tumors (stage IVA), expression was more concentrated and elevated, suggesting a potential role in tumor progression. Although previous studies reported downregulation of ALDH1A2 in HNSC and its association with poor prognosis [29], which contrasts with our differential expression results, this discrepancy may be attributable to limited sample size or sample heterogeneity. Nevertheless, combined with stage-stratified analysis, ALDH1A2 appears to be implicated in tumor progression.

Survival analysis indicated that EVI5 high expression may exert a protective effect, although its expression trend increases in advanced-stage tumors. Prior studies in head and neck-related malignancies (including

laryngeal and glottic squamous cell carcinomas) demonstrated that EVI5 is upregulated and promotes tumor cell proliferation and growth by maintaining cell cycle regulators—stabilizing c-MYC, modulating G1→S transition, and inhibiting APC/C activity [30]. This observation partially conflicts with our survival and differential expression analyses, suggesting that the biological role of EVI5 in HNSC requires further investigation.

LCAT did not show significant differential expression but was significantly associated with DFS. Previous studies indicate that LCAT exhibits context-dependent roles in cancer: it may promote tumor growth in adrenocortical carcinoma (ACC) and colon adenocarcinoma (COAD), while inhibiting progression in low-grade glioma (LGG) and hepatocellular carcinoma (LIHC) [31]. Currently, data on LCAT in HNSC are limited; however, the elevated expression observed in certain advanced-stage samples, combined with its survival association, suggests that LCAT may serve as a potential biomarker for tumor progression.

4.4. Research limitations and prospects

The limitations of this study should be acknowledged. First, the MR analysis employed a broad HNC outcome encompassing multiple tissue types and pathological subtypes, which may have obscured local effects of blood lipids specifically in HNSC. Second, the sample size for differential expression and immune infiltration analyses was limited, potentially affecting the statistical significance of certain genes (e.g., ALDH1A2, EVI5, and LCAT) and leading to discrepancies with previously reported findings. Additionally, this study did not perform systematic functional experiments, nor did it account for potential confounding factors such as environmental exposures and lifestyle habits, thereby limiting the comprehensiveness and depth of causal interpretation. Future studies should incorporate larger-scale clinical cohorts and functional experiments to validate the mechanistic role and clinical potential of ADH1B, thereby providing key targets for the precision prevention and treatment of HNSC in the context of lipid metabolism.

5. Conclusion

This study systematically evaluated the potential causal relationship between circulating lipid-related traits (TC, ApoA-I, and LDL-C) and HNC risk, while exploring the biological mechanisms and clinical implications of lipid-related genetic variants. The study followed a three-step design. First, two-sample MR using publicly available GWAS data showed no significant causal effect of TC, ApoA-I, or LDL-C on HNC risk. Second, SNPs identified from MR were stratified by effect direction and subjected to functional annotation and pathway enrichment. Positive effect group SNPs were enriched in CYP450-mediated drug and xenobiotic metabolism pathways, whereas negative effect group SNPs were enriched in monocarboxylic acid metabolism, alcohol metabolism, and nutrient response pathways, suggesting HNC/HNSCC risk may be modulated by two opposing mechanisms. Third, candidate genes were integrated into multi-omics databases for DE, survival, immune infiltration, and clinical pathological stage analyses. Results showed that ADH1B was downregulated in tumors and may exert a protective effect, indicating its potential as a novel target for tumor immunotherapy. Conversely, FADS1, FADS2, PARP9, and SEMA7A were upregulated and associated with an immunosuppressive TME. Although ALDH1A2, EVI5, and LCAT did not show significant DE, they demonstrated potential prognostic value in OS/DFS and clinical stage analyses.

Disclosure statement

The authors declare no conflict of interest.

References

[1] Zhou T, Huang W, Wang X, et al., 2024, Global Burden of Head and Neck Cancers from 1990 to 2019. iScience, 27(3): 109282.

[2] Barsouk A, Aluru J, Rawla P, et al., 2023, Epidemiology, Risk Factors, and Prevention of Head and Neck Squamous Cell Carcinoma. Medical Sciences (Basel, Switzerland), 11(2): 42.

[3] Jin H, Wang J, Wang Z, et al., 2023, Lipid Metabolic Reprogramming in Tumor Microenvironment: From Mechanisms to Therapeutics. Journal of Hematology & Oncology, 16(1): 103.

[4] Liu R, Wang C, Tao Z, et al., 2025, Lipid Metabolism Reprogramming in Cancer: Insights into Tumor Cells and Immune Cells within the Tumor Microenvironment. Biomedicines, 13(8): 1895.

[5] Cioce M, Arbitrio M, Polerà N, et al., 2024, Reprogrammed Lipid Metabolism in Advanced Resistant Cancers: An Upcoming Therapeutic Opportunity. Cancer Drug Resistance (Alhambra, Calif.), 7: 45.

[6] Liang J, Li L, Li L, et al., 2023, Lipid Metabolism Reprogramming in Head and Neck Cancer. Frontiers in Oncology, 13: 1271505.

[7] Huang Y, Xiao X, Sadeghi F, et al., 2023, Blood Metabolic Biomarkers and the Risk of Head and Neck Cancer: An Epidemiological Study in the Swedish AMORIS Cohort. Cancer Letters, 557: 216091.

[8] Wang S, Wang L, Li H, et al., 2024, Correlation Analysis of Plasma Lipid Profiles and the Prognosis of Head and Neck Squamous Cell Carcinoma. Oral Diseases, 30(2): 329–341.

[9] Wilms T, Boldrup L, Gu X, et al., 2021, High Levels of Low-Density Lipoproteins Correlate with Improved Survival in Patients with Squamous Cell Carcinoma of the Head and Neck. Biomedicines, 9(5): 506.

[10] Feng J, Zhao J, Yang X, et al., 2021, The Prognostic Impact of Preoperative Serum Apolipoprotein A-I in Patients with Esophageal Basaloid Squamous Cell Carcinoma. Cancer Management and Research, 13: 7373–7385.

[11] Elsworth B, Lyon M, Alexander T, et al., 2020, The MRC IEU OpenGWAS Data Infrastructure. bioRxiv, 2020.08.10.244293v1.

[12] McLaren W, Gil L, Hunt SE, et al., 2016, The Ensembl Variant Effect Predictor. Genome Biology, 17(1): 122.

[13] Zhou Y, Zhou B, Pache L, et al., 2019, Metascape Provides a Biologist-Oriented Resource for the Analysis of Systems-Level Datasets. Nature Communications, 10(1): 1523.

[14] Tang Z, Kang B, Li C, et al., 2019, GEPIA2: An Enhanced Web Server for Large-Scale Expression Profiling and Interactive Analysis. Nucleic Acids Research, 47(W1): W556–W560.

[15] Cui H, Zhao G, Lu Y, et al., 2025, TIMER3: An Enhanced Resource for Tumor Immune Analysis. Nucleic Acids Research, 53(W1): W534–W541. https://doi.org/10.1093/nar/gkaf388

[16] Cerami E, Gao J, Dogrusoz U, et al., 2012, The cBio Cancer Genomics Portal: An Open Platform for Exploring Multidimensional Cancer Genomics Data. Cancer Discovery, 2(5): 401–404.

[17] Burgess S, Bowden J, Fall T, et al., 2017, Sensitivity Analyses for Robust Causal Inference from Mendelian Randomization Analyses with Multiple Genetic Variants. Epidemiology (Cambridge, Mass.), 28(1): 30–42.

[18] Malik D, David R, Gooderham N, 2018, Ethanol Potentiates the Genotoxicity of the Food-Derived Mammary Carcinogen PhIP in Human Estrogen Receptor-Positive Mammary Cells: Mechanistic Support for Lifestyle Factors (Cooked Red Meat and Ethanol) Associated with Mammary Cancer. Archives of Toxicology, 92(4): 1639–1655.

[19] An Y, Chen X, Yang Y, et al., 2018, LncRNA DLX6-AS1 Promoted Cancer Cell Proliferation and Invasion by

Attenuating the Endogenous Function of miR-181b in Pancreatic Cancer. Cancer Cell International, 18: 143.

[20] National Toxicology Program, 2021, 15th Report on Carcinogens. National Toxicology Program, Research Triangle Park (NC). Acetaldehyde: CAS No. 75-07-0, visited on June 12, 2025, https://www.ncbi.nlm.nih.gov/books/NBK590821/?utm_source=chatgpt.com

[21] Creamer K, Larsen E, Lawrence J, 2022, ZNF146/OZF and ZNF507 Target LINE-1 Sequences. G3 (Bethesda, Md.), 12(3): jkac002.

[22] Yukawa Y, Muto M, Hori K, et al., 2012, Combination of ADH1B2/ALDH22 Polymorphisms Alters Acetaldehyde-Derived DNA Damage in the Blood of Japanese Alcoholics. Cancer Science, 103(9): 1651–1655.

[23] Chien H, Tsai C, Young C, et al., 2023, Single-Nucleotide Polymorphism at Alcohol Dehydrogenase 1B: A Susceptible Gene Marker in Oro-/Hypopharyngeal Cancers from Genome-Wide Association Study. Cancer Medicine, 12(18): 19174–19187.

[24] Heravi G, Jang H, Wang X, et al., 2022, Fatty Acid Desaturase 1 (FADS1) Is a Cancer Marker for Patient Survival and a Potential Novel Target for Precision Cancer Treatment. Frontiers in Oncology, 12: 942798.

[25] Gong Q, Li H, Song J, et al., 2023, LncRNA LINC01569 Promotes M2 Macrophage Polarization to Accelerate Hypopharyngeal Carcinoma Progression through the miR-193a-5p/FADS1 Signaling Axis. Journal of Cancer, 14(9): 1673–1688.

[26] Xuan Y, Wang H, Yung M, et al., 2022, SCD1/FADS2 Fatty Acid Desaturases Equipoise Lipid Metabolic Activity and Redox-Driven Ferroptosis in Ascites-Derived Ovarian Cancer Cells. Theranostics, 12(7): 3534–3552.

[27] Saleh H, Liloglou T, Rigden D, et al., 2024, KH-Like Domains in PARP9/DTX3L and PARP14 Coordinate Protein-Protein Interactions to Promote Cancer Cell Survival. Journal of Molecular Biology, 436(4): 168434.

[28] Liu Z, Meng X, Zhang Y, et al., 2024, FUT8-Mediated Aberrant N-Glycosylation of SEMA7A Promotes Head and Neck Squamous Cell Carcinoma Progression. International Journal of Oral Science, 16(1): 26.

[29] Seidensaal K, Nollert A, Feige A, et al., 2015, Impaired Aldehyde Dehydrogenase 1 Subfamily Member 2A-Dependent Retinoic Acid Signaling Is Related with a Mesenchymal-Like Phenotype and an Unfavorable Prognosis of Head and Neck Squamous Cell Carcinoma. Molecular Cancer, 14: 204.

[30] Mao C, Zhou X, Jiang Y, et al., 2020, The Evi5 Oncogene Promotes Laryngeal Cancer Cells Proliferation by Stabilizing c-Myc Protein. Cancer Cell International, 20: 44.

[31] Gao M, Zhang W, Li X, et al., 2025, LCAT in Cancer Biology: Embracing Epigenetic Regulation, Immune Interactions, and Therapeutic Implications. International Journal of Molecular Sciences, 26(4): 1453.